

## Alpha heating in ITER L-mode and H-mode plasmas

R.V. Budny

Princeton Plasma Physics Laboratory, Princeton, NJ 08543, USA

**1. Introduction.** There are many uses of predictions of ITER plasma performance. One is assessing requirements of different plasma regimes. For instance, what current drive and control are needed for steady state. The heating, current drive, and torque systems planned for initial DT operation are negative ion neutral beam injection (NB), ion cyclotron resonance (IC), and electron cyclotron resonance (EC). Which combinations of heating are optimal. What are benefits of the torques, current drive, and fueling using NB. What are the shine-through power and optimum voltage for the NB? What are optimal locations and aiming of the EC launchers? Another application is nuclear licensing (e.g. System integrity, how many neutrons).

One important application is generating inputs for design of diagnostic systems and for theoretical studies. An example of the later is Alfvén Eigenmode and AE-induced loss of fast ions. The beam ion distribution can either enhance or reduce the alpha pressure drive of the AE instability [1]. The AE instability can cause dangerous amounts of fast ion losses. A quasi-linear model [2] indicates that central  $\beta_\alpha$  values as low as 1% can induce fast ion loss fractions at dangerous levels of 5% in standard shear ITER plasmas.

**2. PTRANSPI.** This paper describes PTRANSPI [3-6] predictive modeling for ITER. Time-dependent, integrated, self-consistent predictions are generated for baseline cases with toroidal field = 5.3 T, and plasma current ramped to 15 MA. Effects of sawtooth mixing and alpha ash accumulation are modeled. Details are in [3,5]. An assumed flat electron density profile  $n_e$  is ramped to a Greenwald fraction of 0.85. Various combinations of external heating by NB, IC, and EC [5,6] are assumed to start half-way up the density ramp with the planned total auxiliary heating power of  $P_{ext}=73$  MW. After 50 s  $P_{ext}$  is reduced to 50 MW to increase  $Q_{DT}$ . Time evolutions for one of the heating cases are shown in FIG. 1.

The time evolution of plasma temperatures and toroidal rotation  $v_\phi$  are predicted assuming boundary values using the GLF23 model [7]. Conservatively low boundary temperatures ( $\simeq 0.6$  keV) and  $v_\phi$  ( $\simeq 400$  Rad/s) are assumed.

Two alternative options are used to predict  $v_\phi$  and the  $E \times B$  flow shearing rate induced by the NB torques in order to include a range of predictions of flow-shear turbulence transport suppression. Option 1 assumes that the momentum transport coefficient  $\chi_\phi$  is half the energy transport coefficient  $\chi_i$  predicted consistently with the GLF23-predicted temperatures. Option 2 uses GLF23 to predict both the temperatures and directly  $v_\phi$ . Significantly higher  $v_\phi$  and flow-shearing rates are predicted. Central  $v_\phi$  rates are shown in FIG. 2. With Option 1 flow shearing does not affect significantly the energy transport,

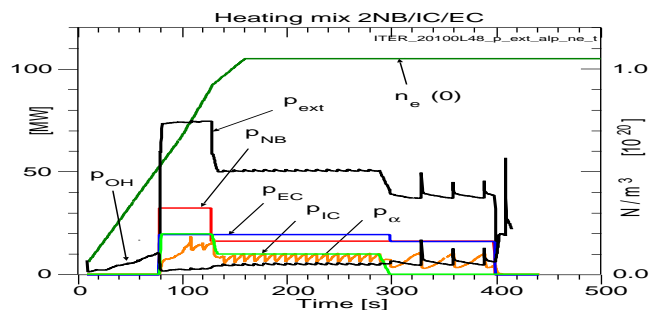


FIG. 1: Central  $n_e$ , external heating, and alpha heating for an L-mode case with one of the heating mixes. A sawtooth period of 10s is assumed with Kadomtsev-like helical mixing if  $q(0) < 1.0$ .

and with Option 2, significant reduction of energy transport is predicted.

The  $L \rightarrow H$  power threshold  $P_{L \rightarrow H}$  is assumed to be proportional to a fit  $P_{Martin}$  [8] to an ITPA database. Since this scaling decreases with decreasing  $n_e$ , it might be beneficial for ITER to start NB injection early, as shown in [FIG. 1](#). Full-power beam injection can not start at very low density since the beam shine-through could damage the first wall. Also  $P_{L \rightarrow H}$  is observed to increase at very low  $n_e$  in some tokamaks.

**3. L-mode.** The full external power planned,  $P_{ext} = 73$  MW is sufficient to achieve the H-mode with  $P_{Martin}$  scaling. However, since there is not a generally accepted physics-based theory for  $L \rightarrow H$ , it is unclear how much auxiliary heating power will be required to achieve an H-mode in ITER. Thus it is interesting to predict alpha heating in ITER L-mode DT plasmas since  $P_\alpha$  will enhance  $P_{ext}$ , and  $P_\alpha + P_{ext}$  might be sufficient to achieve H-mode confinement. Here the L-mode is simulated by scaling  $P_{Martin}$  by factors of two or three to prevent the  $L \rightarrow H$  transition.

In the case of high  $P_{L \rightarrow H}$  and Option 1 for  $v_{tor}$  and flow shear, the ion temperature  $T_i$  predicted for various heating mixes are shown in [FIG. 3](#). Plots of the total thermal plasma  $P_{plasma-heat}$  and total alpha heating  $P_\alpha$  using Option 1 are shown in [FIG. 4-a,b](#)). The peak  $P_\alpha$  is  $\sim 17$  MW (for the mix with full NB) and decreases after 50s (at 130 s) when  $P_{ext}$  is reduced.

With Option 2 first consider the case where  $P_{L \rightarrow H}$  is higher than  $P_{ext}$  for all the heating mixes. Much higher  $v_{tor}$  (shown in [FIG. 3-b](#)) and central  $T_i$  about twice those in [FIG. 3](#) are predicted. The boundary values for temperatures and  $v_\phi$  are the same as those used for Option 1. Plots of  $P_{plasma-heat}$  and  $P_\alpha$  are shown in [FIG. 4-c,d](#)). The alpha heating reaches 60 MW in the heating mix with full NB power. The large range of predictions from Option 1 and 2 indicates effects of large uncertainties in the physics.

Next consider Option 2 with  $P_{L \rightarrow H}$  scaled up a factor of two. Heating mixes with NB transition to H-mode and the others do not. In the L-mode, the temperatures and  $v_{tor}$  are the same as the results for Option 2 above with higher  $P_{L \rightarrow H}$ . Plots of  $P_{plasma-heat}$  and  $P_\alpha$  are shown in [FIG. 4-e,f](#)). When the plasma transitions to H-mode the PEDESTAL module [9] in PTRANSP is used to predict the pedestal width and pressure at the top of the pedestal. Since the  $n_e$  profile is prescribed, the pressure determines the pedestal temperatures used as boundary values for GLF23. These values can be scaled in PTRANSP, and for these runs the flat top values of both the ion and electron temperatures are 4.6 keV.

**4. H-mode.** For the H-mode predictions GLF23 is used for the plasma temperatures, but not for  $v_\phi$ . The flow shear is computed using Option 1. With the NB torques,  $v_\phi$  is predicted to be relatively low (central values  $\simeq 6$  kRad/s) and the flow-shearing rate is predicted to have little effect on the GLF23-predicted temperatures. The assumed external heating mix is very similar to that shown in [FIG. 1](#).

The values of  $\beta_{n-ped}$  are scanned. Profiles of  $P_\alpha$  are shown in [FIG. 5-a](#)), and values of  $Q_{DT}$  are shown in [FIG. 5-b](#)). Parameters at two times are summarized in [FIG. 6](#) when  $P_{ext}=73$  and 48MW. These plots are approximately linear in  $\beta_{n-ped}$  contrary to the quadratic dependence seen with simulations that do not include the effects of alpha ash accumulation (that becomes more acute at higher fusion power), or effects of changes in the heating profiles as the plasma temperatures change. Both effects are included here.

There are several mechanisms that could impose upper limits on  $\beta_{n-ped}$ , and thus the H-mode per-

formance. One is NTM activity. Another is Type I ELM activity that could deposit too much localized energy of first walls. Another is fast ion loss that also could deposit too much localized energy of first walls. NTM activity is associated with high values of  $\beta_n$  that increase with  $\beta_{n-ped}$ . A peeling-balloonning model for ELMs [10] indicates that values of  $\beta_{n-ped}$  above  $\simeq 0.8$  are dangerous. AE-induced alpha loses appear to be excessive if  $\beta_\alpha(0)$  is above 1% (the value predicted with  $T_{ped} \simeq 5.5$ keV). Thus to reach the goal of  $Q_{DT}=10$ ,  $P_{ext}=73$ MW appears too high, but 48MW appears promising. The upper limits of  $P_\alpha$  appear to be about 70-80MW at both  $P_{ext}=73$  and 48MW. It is curious that the upper limit predicted for the L-mode with  $P_{ext}=73$ MW and the optimistic Option 2, 60MW is close to the H-mode limit predicted with the pessimistic Option 1.

**5. Prospects.** There are many uncertainties in ITER predictions. Besides the uncertainties in  $P_{L \rightarrow H}$ ,  $\beta_{n-ped}$ , and flow-shearing effects addressed above, there are many others not addressed here: fast ion anomalous losses, MHD, density profiles including ash transport and recycling. Experiments in ITER will most probably discover many unexpected phenomena.

Developments of PTRANSP by the teams especially at PPPL and Lehigh were crucial for this research. Notice: This manuscript has been authored by Princeton University under Contract Number DE-AC02-09CH11466 with the U.S. Department of Energy. The publisher, by accepting the article for publication acknowledges, that the United States Government retains a non-exclusive, paid-up, irrevocable, world-wide license to publish or reproduce the published form of this manuscript, or allow others to do so, for United States Government purposes.

**References.** [1] N.N.Gorelenkov, H.L.Berk, R.V.Budny, Nucl. Fusion **45**, 226 (2005). [2] N.N.Gorelenkov, private communication [3] R.V.Budny, R.Andre, G.Bateman, F.Halpern, *et al.*, Nucl. Fusion **48**, 075005 (2008). [4] F.D.Halpern, A.H.Kritz, G.Bateman, A.Y.Pankin, R.V.Budny, and D.C.McCune, Phys. of Plasmas **15**, 062505 (2008). [5] R.V.Budny, Nucl. Fusion **49**, 085008 (2009). [6] R.V.Budny, PPPL Report-4590, (2011). [7] R.E.Waltz, G.M.Staebler, W.Dorland, G.W.Hammett, *et al.*, Phys. Plasmas **4** 2482 (1997). [8] Y.Martin, J. of Physics Conference Series **123** (2008) 012033. [9] T.Onjin, G.Bateman, A.H.Kritz, and G.Hammett, Plasma Phys. Controlled Fusion **45** 1939 (2003). [10] P.B.Snyder, R.J.Groebner, A.W.Leonard, T.H.Osborne, and H. R. Wilson, Phys. of Plasmas **16**, 056118 (2009).

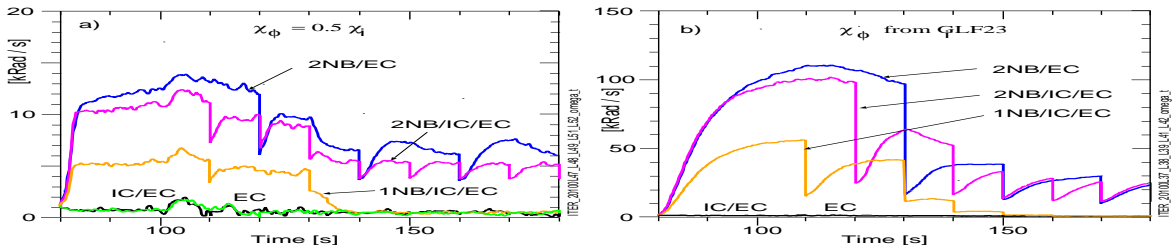


FIG. 2: Central toroidal rotation for different heating mixes predicted assuming low temperatures and rotation at the boundary, and  $P_{plasma-heat} < P_{L \rightarrow H}$  and NB torques with a)  $\chi_\phi = 0.5\chi_{i-GLF23}$ ; b)  $\chi_\phi = \chi_{i-GLF23}$ .

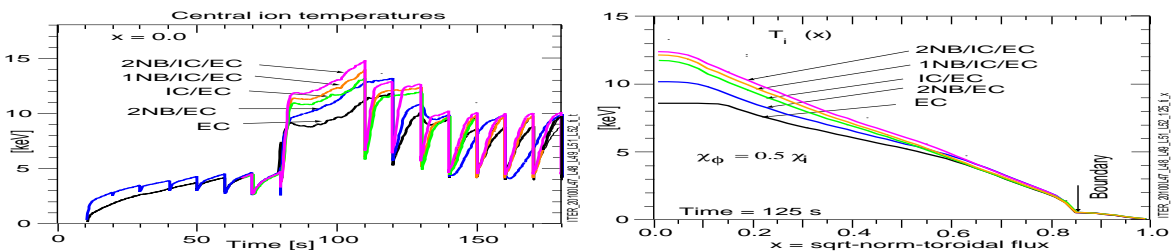


FIG. 3: Ion temperatures predicted for different heating mixes using  $\chi_\phi = 0.5\chi_{i-GLF23}$ , low  $T_{ped}$ , and  $P_{plasma-heat} < P_{L \rightarrow H}$ .

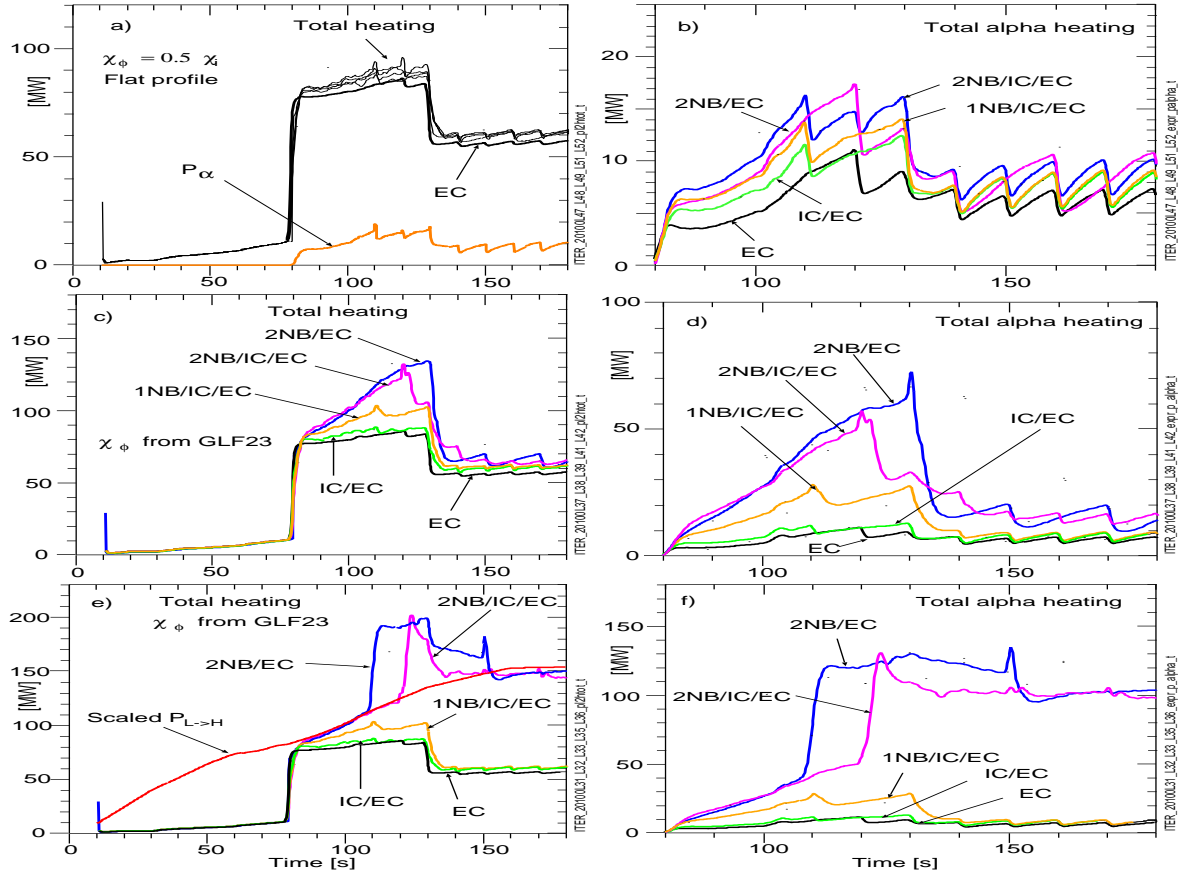


FIG. 4: Total heating and alpha with five external heating mixes; a,b) Option 1 with  $P_{\text{heat}} < P_{L \rightarrow H}$ ; (to prevent the H-mode); c,d) Option 2 with  $P_{\text{heat}} < P_{L \rightarrow H}$ ; (to prevent the H-mode); e,f) Option 2 with  $P_{\text{heat}} = 2 \times P_{L \rightarrow H}$  which allows the heating mixes with NB to achieve H-mode during the density ramp

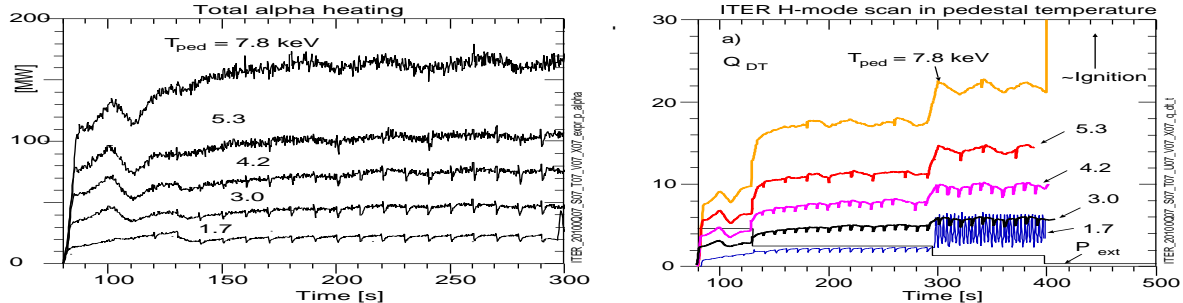


FIG. 5: Total alpha heating and  $Q_{DT}$  for different assumptions for the pedestal temperature.

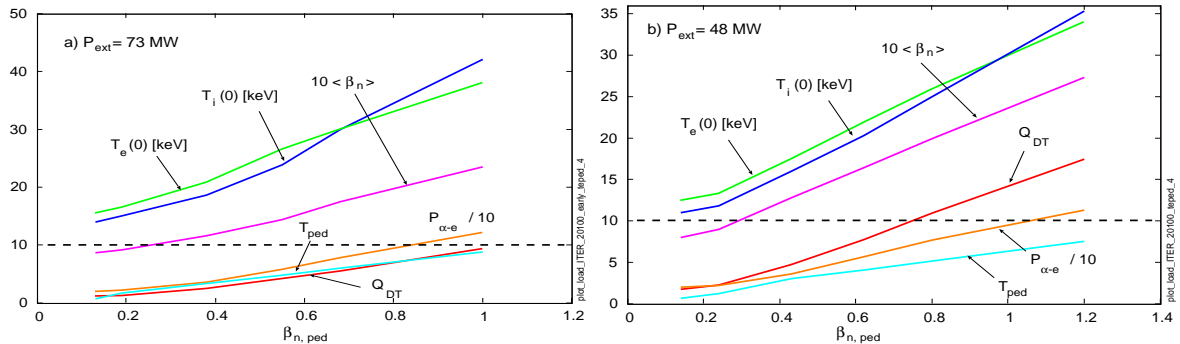


FIG. 6: Scaling of various parameters with  $\beta_{n-ped}$  with a)  $P_{\text{ext}} = 73 \text{ MW}$ , and b)  $48 \text{ MW}$ .